Radiation-Enhanced Annealing of Vacancy–Oxygen Defects in Cz n-Si: Features of the Experiment, Factor of the Radiation Ionization, and a Possible Annealing Mechanism

Mykola Kras'ko, Andrii Kolosiuk,* Vasyl Povarchuk, and Vasyl Voitovych

The results of the detailed study of the accumulation and/or annealing of vacancy–oxygen (VO) complexes kinetics in the Czochralski-grown n-type silicon (Cz n-Si) are presented. The samples are irradiated by electron beam pulses of different energies and intensities (J) at VO effective annealing temperatures ($>300\,°C$). It is shown that: 1) upon high-temperature (so-called "hot") irradiation Cz n-Si at temperatures $>300\,°C$, J can significantly stimulate VO annealing and a maximum concentration of accumulated VO defects ($[VO]_{max}$, when the rates of formation and simultaneous annealing of VO complexes are equal) increases with increasing J and decreases with increasing irradiation temperature. Accelerated annealing of VO slows down sharply the growth rate of $[VO]_{max}$ as a function of J; 2) the VO defects introduced into Cz n-Si at room temperature can also be annealed faster if the annealing is accompanied by additional electron irradiation of a certain intensity. It has been established that the radiation-accelerated annealing of VO is characterized by a decrease in the activation energy from ≈ 1.7 to $\approx 0.5\,eV$ due to radiation ionization of the Si crystal. A model of the enhanced VO annealing process is proposed.

1. Introduction

The properties of crystalline silicon, which is the main material in the modern semiconductor device industry, are determined by the variety and nature of impurities and defects present. These impurities and defects of a silicon crystalline structure are introduced at different technological stages, namely, during the growth of Si, in the processes of manufacturing Si devices and also their operation in both normal and extreme conditions. Radiation-induced defects in silicon can significantly affect the properties of the Si material and devices. To a large extent, the formation of these defects causes radiation damage of silicon devices operating in radiation conditions, for example, in the space environment, in applications related to nuclear experiments, nuclear power, and medicine. In this regard, increasing the radiation resistance of both materials and devices is an important scientific and technological task. On the other hand, irradiation with various particles is used to control the behavior of silicon device parameters, to modify the silicon material, or is part of manufacturing processes. Examples are ion implantation, electron beam deposition, neutron transmutation doping of silicon, and the use of irradiation to control the minority carrier lifetime in silicon power devices. All these processes also lead to the formation of various radiation-induced defects. Usually, appropriate heat treatments are then carried out to stabilize the desired effects of irradiation and reduce the harmful ones.

The radiation effects induced by high-temperature irradiation of silicon materials and devices are noticeably different from those obtained during room temperature (RT) irradiation or irradiation at RT and subsequent annealing at higher temperatures.[1–14] In particular, a number of interesting effects were observed in silicon irradiated at elevated temperatures. The 2 MeV electron irradiation of Si at 700 °C leads to an acceleration of the in-diffusion of platinum, which is used to reduce the minority carrier lifetime in Si power diodes.[2] The generation rate of oxygen-related thermal donors in Czochralski-grown n-type silicon (Cz n-Si) increases under the influence of 1 MeV electron irradiation at 450 °C.[3,4] This can be evidence of the radiation-stimulated diffusion of oxygen or the formation of a larger number of thermodonor nuclei during hot electron irradiation. Such a point of view is consistent with the fact that hot electron irradiation of Cz n-Si in the 320–500 °C range increases the generation efficiency of oxygen dimers (O_{2i}), which significantly affect the formation of radiation and thermal defects in silicon.[5,6]

Also, new deep acceptors were revealed in high-temperature irradiated n-Si, which can be related to higher-order vacancy–oxygen complexes (V_mO_n, where $m, n \geq 1$).[2,4,7–11] In as-grown Si crystals, interstitial oxygen atoms (O_i) are the main technological impurity, which is electrically neutral and immobile at RT. However, in irradiated or irradiated and annealed silicon, various kinds of VO-related complexes (V_mO_n, where $m, n \geq 1$) are formed.[5,6,15–29] Some of them (e.g., VO, V_2O, V_3O) are electrically active, and the dominant one among them is the VO complex (or A-center), formed by the interaction of a mobile vacancy and interstitial oxygen (the reaction $V + O_i \rightarrow VO$). Long-term scientific and technological interest in VO defects is due to

M. Kras'ko, A. Kolosiuk, V. Povarchuk, V. Voitovych
Laboratory of Radiation Technologies
Institute of Physics of the NAS of Ukraine
46 Prospekt Nauky, Kyiv 03028, Ukraine
E-mail: kolosiuk@iop.kiev.ua

The ORCID identification number(s) for the author(s) of this article can be found under https://doi.org/10.1002/pssa.202400900.

their properties, which are well investigated using different techniques, namely, electron paramagnetic resonance studies, infrared absorption spectroscopy, Hall effect measurements, deep-level transient spectroscopy, and carrier lifetime measurements.[2,5–11,15–18,20,23–25,29–36] In standard-doped Cz silicon, the oxygen concentration ($[O_i] \approx 10^{17}$–10^{18} cm^{-3}) is much more than concentrations of other impurities, and after the irradiation with gamma quanta (^{60}Co) or few MeV electrons at RT, the VO concentration is usually much higher than the concentration of other vacancy-related defects (e.g., vacancy–phosphorus complex (E-center)).[7,11,34] Having an acceptor level of E_c 0.17 eV in the bandgap of silicon (E_c is the conduction band edge), VO defects are effective recombination centers in Cz n-Si at RT and also at higher irradiation temperatures.[11,34–37] These defects can also affect the mechanical properties of irradiated silicon.[21] The VO complexes are stable up to $\approx$300 °C.[6,20,24,34] Upon annealing, they are largely transformed into higher order V_mO_n complexes ($m, n \geq 1$), which are also of technological interest and are less researched.[5–7,11,17] The results of experiments on hot irradiation of silicon at temperatures $\geq$300 °C indicate that VO complexes remain the dominant radiation-induced defects.[1,2,4–11] In this case, the obtained concentration of VO is determined by the efficiency of two simultaneous processes—the formation of VO defects and their annealing. This fact made it possible to investigate the process of free vacancy generation in n-Si during electron irradiation at high temperatures, up to 633 K.[38] We have previously established that VO accumulation in Cz n-Si at the temperature of their effective annealing (360 °C) depends on the intensity of electron irradiation.[1,39] At the same time, it is established that J does not affect the formation efficiency of VO complexes, but accelerates their annealing by more than an order of magnitude. In general, studying the influence of the intensity of irradiation on the operation of silicon devices is an important task.[40]

In the present article, the experimental features and reasons for accelerated annealing of VO complexes in Cz n-Si under the simultaneous action of two factors, namely, the intensity of electron irradiation and the high temperature of the samples during irradiation, are investigated in detail. For this purpose, the kinetics of accumulation and/or annealing of VO complexes were experimentally obtained and theoretically analyzed for different temperatures, intensities, and energies of electron irradiation. The mechanism of the influence of ionizing radiation on the annealing of VO complexes in Cz n-Si is proposed.

2. Results and Discussion

2.1. Radiation-Enhanced Annealing of VO Defects in Cz n-Si: Experimental Results

2.1.1. High-Temperature (Hot) Electron Irradiation

Figure 1 shows dependences of the VO concentration ([VO]) in Cz n-Si on the time (a) and the fluence (b) of hot irradiation with 1 MeV electrons at 347, 360, 450, and 535 °C for different irradiation intensities. Together, these dependences allow a detailed analysis of the influence of J on the kinetics of accumulation VO defects, namely, [VO](t)—on the accumulation rate (d[VO]/dt) and [VO](Φ)—on the accumulation efficiency (d[VO]/$d\Phi$) (where $\Phi = J \times t$). In general, the d[VO]/$d\Phi$ value is equal to the VO concentration formed by one electron of the irradiation beam, which can be used to quantitatively compare the effects at different irradiation intensities.

From the experimental data in Figure 1, we note the following: 1) the VO accumulation has the form of a curve with saturation and occurs qualitatively the same at all J and irradiation temperatures (T_{irr}). At the same time, the efficiency of VO accumulation in the initial stages of [VO](Φ) in Figure 1b is independent of J and is equal to d[VO]/$d\Phi(t \to 0) = (7.9 \pm 0.3) \times 10^{-2}$ cm^{-1}. Accordingly, the initial rate of VO accumulation in Figure 1a is a linear function of J, d[VO]/$dt(t \to 0) = J \times d$[VO]/$d\Phi(t \to 0)$; 2) **Table 1** presents the values of the maximum (at saturation) concentrations of VO defects determined from
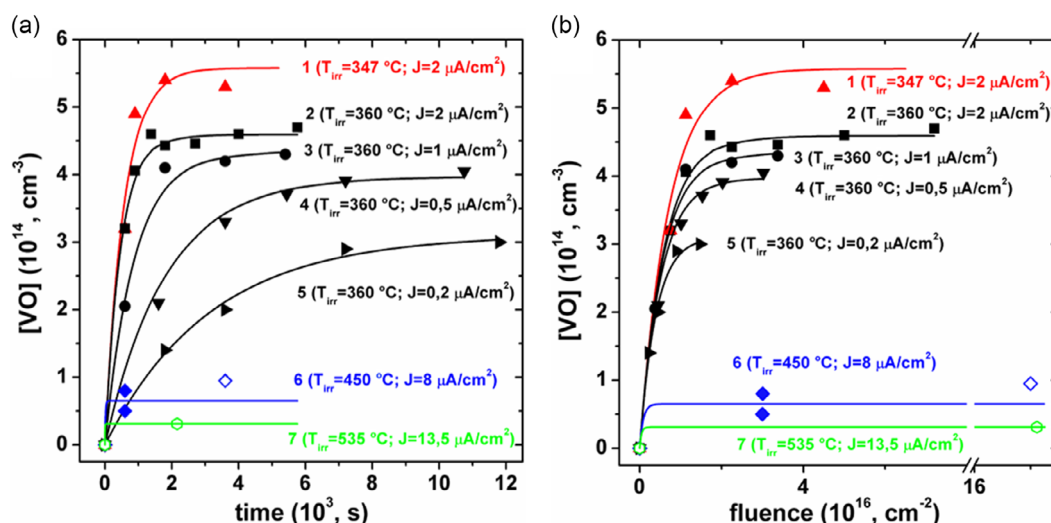

Figure 1. Dependences of the VO concentration on a) the irradiation time and b) the fluence of hot irradiation with 1 MeV electrons at different temperatures and intensities of irradiation. Symbols—experimental data (solid symbols—samples with $[P] \approx 1 \times 10^{15}$ cm^{-3}; open symbols—samples with $[P] \approx 2 \times 10^{16}$ cm^{-3}); lines—description using Equation (3) (see details in the text below).

Table 1. Values of the $[VO]_{max}$ for dependences in Figure 1, which corresponds to different conditions of hot irradiation with 1 MeV electrons.

Comments	Conditions of hot irradiation		Concentration of VO defects at saturation	Concentration of phosphorus in samples
	T_{irr} [°C]	J [μA cm^{-2}]	$[VO]_{max}$ [×10^{14} cm^{-3}]	[P] [×10^{15} cm^{-3}]
Curve 1	347	2	5.6	≈1
Curve 2	360	2	4.6	
Curve 3	360	1	4.3	
Curve 4	360	0.45	4.1	
Curve 5	360	0.2	3.1	
Curve 6	450	8	0.5; 0.8	
Curve 6	450	8	0.95	≈20
Curve 7	535	13.5	0.3	

the dependences in Figure 1. From Table 1 and Figure 1, we observe the following features of the influence of J and T_{irr} on the $[VO]_{max}$: curves 2–5—the $[VO]_{max}$ slowly increases with increasing J from 0.2 to 2 μA cm^{-2} at a constant $T_{irr} = 360$ °C; curves 1 and 2—the $[VO]_{max}$ decreases if the T_{irr} increases from 347 to 360 at a constant $J = 2$ μA cm^{-2}. This trend persists when the T_{irr} is increased to 450 °C (curve 6) and 535 °C (curve 7) even with a significant increase in J to 8 and 13 μA cm^{-2}, respectively. Curve 6—the $[VO]_{max}$ is slightly more (by ≈30%) in samples with a higher level of phosphorus doping, which are irradiated at 450 °C.

We investigated the kinetics of VO accumulation in Figure 1 in order to quantitatively assess the efficiency of the processes of generation and annealing of VO defects during their accumulation depending on the J. For convenience, we analyzed the dependences for samples with a phosphorus doping level of ≈10^{15} cm^{-3} (curves 1–6 in Figure 1). In these samples, the

concentration of $[O_i]$ exceeds that of other impurities and radiation-induced defects by at least an order of magnitude, and therefore it can be considered that all vacancies (V) after the dissociation of the Frenkel pairs form VO complexes (V + O$_i$ → VO).

In the case of hot irradiation at $T_{irr} > 300$ °C, VO generation and their annealing with the time constant τ occur simultaneously. Therefore, the system of kinetic equations consists of two equations that describe the formation and annealing of V and VO

$$
\begin{cases}
\dfrac{d[V](t)}{dt} = \lambda_V - \chi_{VO}[V](t)[O_i] \\
\dfrac{d[VO](t)}{dt} = \chi_{VO}[V](t)[O_i] - \dfrac{[VO](t)}{\tau}
\end{cases}
\tag{1}
$$

where λ_V is the free vacancies generation rate, χ_{VO} is the capture constant of V by oxygen. The τ^{-1} is the temperature-dependent rate constant of VO defect annealing, which is described by the relation

$$
\frac{1}{\tau} = \nu \times \exp\left(-\frac{E_a}{kT}\right)
\tag{2}
$$

where ν is the frequency factor, E_a is the activation energy, k is the Boltzmann constant, and T is the absolute temperature.

In ref. [1], we showed that the solution of Equation (1) (initial conditions: $d[V]/dt = 0$ and $[VO]|_{t=0} = 0$) gives the following analytical expression for the dependence of the accumulated VO concentration at $T_{irr} > 300$ °C on the hot irradiation time (t_{irr})

$$
[VO](t) = \lambda_V \tau \times \left(1 - \exp\left(-\frac{t_{irr}}{\tau}\right)\right)
\tag{3}
$$

Solid lines in Figure 1 represent the results of the simulation of experimental data by Equation (3). For solid curve 1 ($T_{irr} = 347$ °C), we obtained that $\lambda_V/J = 7.9 \times 10^{-2}$ cm^{-1} and $\tau = 565$ s. **Figure 2**a shows calculated (best fit between experiment and simulation) values of λ_V and τ as a function of J at
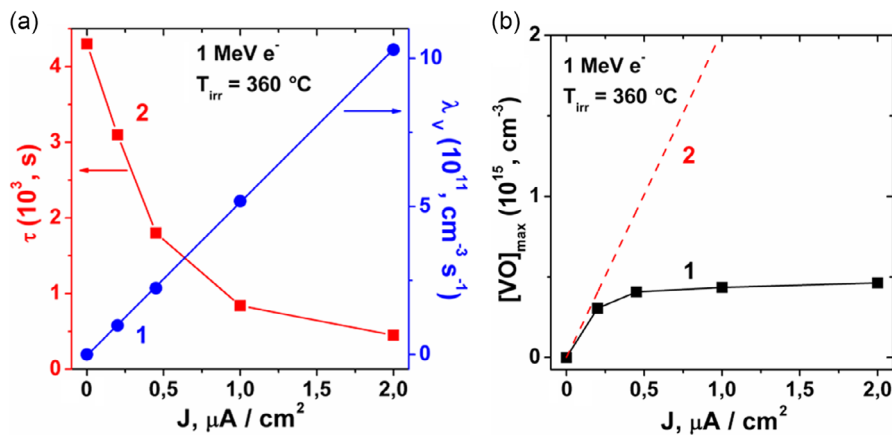

Figure 2. a) Calculated values of λ_V (curve 1) and τ (curve 2) as a function of J for 1 MeV electron irradiation at 360 °C. Symbols—results of the description of the experimental data Figure 1 by Equation (3). The solid line for curve 1 is a linear approximation. b) The $[VO]_{max}$ as a function of J: curve 1—experimental data from Figure 1; curve 2—calculated by Equation (4) for the case when $[VO]_{max}$ does not depend on J ($\tau = 4.3 \times 10^3$ s; $\lambda_V/J = 7.9 \times 10^{-2}$ cm^{-1}).

$T_{irr} = 360\,°C$, which characterize the processes of generation and annealing of VO defects during their accumulation. From Figure 2a, 1) the λ_V increases linearly with increasing J (curve 1). And at the same time, the efficiency of vacancies formation (by one electron of irradiation) is a constant value of $\lambda_V/J = (7.9 \pm 0.2) \times 10^{-2}\,cm^{-1}$ (the same for $T_{irr} = 347\,°C$), that is, it does not depend on J; 2) the τ strongly (almost by an order of magnitude) decreases with increasing J (curve 2; the value of τ for $J = 0$ on this dependence corresponds to irradiation at RT followed by annealing at $360\,°C$), which means radiation-accelerated annealing of VO defects.

At the initial stage of VO accumulation, the condition $t_{irr} \ll \tau$ for Equation (3) must be met. Then from Equation (3), we obtain that $[VO](t \to 0) = \lambda_V \times t_{irr}$ and, accordingly, $d[VO]/dt(t \to 0) = \lambda_V$ and $d[VO]/d\Phi(t \to 0) = \lambda_V/J$. Thus, the initial stage of VO accumulation in Figure 1 is determined only by the process of VO formation due to the generation of free V.

The stage of saturation on the VO accumulation dependences in Figure 1 is a consequence of the equality of the rates of formation and annealing of VO defects, and the condition $t_{irr} \gg \tau$ in Equation (3) is also fulfilled. Then we have

$$[VO]_{max} = \lambda_V \times \tau \tag{4}$$

Solid lines in Figure 1 for $T_{irr} = 450\,°C$ (curve 6) and $T_{irr} = 535\,°C$ (curve 7) correspond to the calculation by Equation (3), provided that $\lambda_V/J = 7.9 \times 10^{-2}\,cm^{-1}$ for both irradiation temperatures, and the values of τ are 16.5 and 4.7 s for T_{irr} of 450 and 535 °C, respectively. These τ values were determined using Equation (4), assuming that the experimental VO concentrations for these irradiation temperatures correspond to the maximum concentrations (at saturation).

Figure 2b shows dependences of the $[VO]_{max}$ on the J of 1 MeV electron hot irradiation at 360 °C: curve 1—experimental data from Figure 1; curve 2—calculated by Equation (4) for the case when $[VO]_{max}$ does not depend on J ($\tau = 4.3 \times 10^3\,s$; $\lambda_V/J = 7.9 \times 10^{-2}\,cm^{-1}$). At $J > 0.2\,\mu A\,cm^{-2}$, the growth rate of the experimental dependence $[VO]_{max}(J)$ (curve 1) slows down and is much lower compared to the calculation one (curve 2). It is obvious that accelerated annealing of VO complexes is the cause for this behavior of the experimental dependence $[VO]_{max}(J)$. Figure 2a shows that $\tau(J)$ decreases much more strongly than $\lambda_V(J)$ increases. According to Equation (4), the growth rate of $[VO]_{max}(J)$ should decrease, which we observe in the experiment (curve 1 in Figure 2b).

Thus, during hot electron irradiation of samples at temperatures $>300\,°C$, which leads to the simultaneous generation and annealing of VO defects, the irradiation intensity can significantly stimulate their annealing and, accordingly, affect the accumulation of VO complexes in silicon.

2.1.2. Irradiation at RT and Subsequent Annealing

Experiments on the annealing of VO defects introduced by irradiation in silicon at RT show that the kinetics of their annealing in the temperature range 300–500 °C has the same activation energy $E_a \approx 1.7 \pm 0.2\,eV$.[6,34,35,41] Without determining the annealing mechanism of VO defects, the corresponding kinetic equation for VO annealing is as follows

$$\frac{d[VO](t)}{dt} = -\frac{[VO](t)}{\tau} \tag{5}$$

The solution of Equation (5) with the initial condition $[VO]|_{t=0} = [VO]_{RT}$ ($[VO]_{RT}$—the initial VO concentration in samples after irradiation at RT) gives an expression to describe the annealing kinetics of VO

$$[VO](t) = [VO]_{RT} \times \exp\left(-\frac{t}{\tau}\right) \tag{6}$$

where t is the time of annealing.

Figure 3 shows the logarithm of the normalized VO concentration in Cz n-Si ($[P] \approx 1 \times 10^{15}\,cm^{-3}$) irradiated with 1 MeV electrons at RT versus time during isothermal annealing at temperatures between 347 and 450 °C. The experimental data (symbols) in Figure 3 were linearly approximated (solid lines) to determine the VO annealing rate constant τ^{-1} (see Equation (6)). Using the obtained values of τ^{-1} and Equation (2), we calculated that the normal annealing of VO complexes has activation energy E_a in the range $\approx 1.70–1.72\,eV$ and frequency factor ν in the range $\approx(7.5–11.5) \times 10^9\,s^{-1}$. These values are in good agreement with those reported previously in the literature.[6,34]

2.1.3. Annealing With and Without Additional Irradiation

Also, the radiation-enhanced annealing of VO defects introduced in Cz n-Si at RT is possible if the samples are additionally irradiated with electrons during annealing. We observed this effect under two conditions. The first condition is the use of electron irradiation with $J > 0.2\,\mu A\,cm^{-2}$ (see curve 2 in Figure 2a). The second condition for observing radiation-enhanced annealing is a high initial concentration of defects. Simultaneously with the annealing of VO previously introduced at RT, the formation and annealing of VO occur due to additional hot irradiation with electrons. For this case, solving Equation (1) with initial conditions
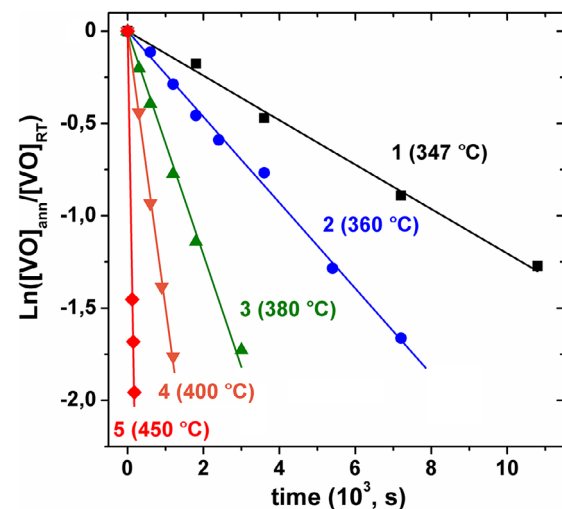

Figure 3. The logarithm of the normalized VO concentration in Cz n-Si ($[P] \approx 1 \times 10^{15}\,cm^{-3}$) irradiated with 1 MeV electrons at RT versus time during isothermal annealing at temperatures between 347 and 450 °C. $\Phi = 8 \times 10^{15}\,cm^{-2}$ and $[VO]_{RT} \approx 5.4 \times 10^{14}\,cm^{-3}$.

$d[V]/dt = 0$ and $[VO]|_{t=0} = [VO]_{RT}$, we obtain the following dependence of the [VO] on the time of radiation-heat treatment (t)

$$[VO](t) = \lambda_V \tau \times \left(1 - \exp\left(-\frac{t}{\tau}\right)\right) + [VO]_{RT} \times \exp\left(-\frac{t}{\tau}\right) \quad (7)$$

As can be seen from Equation (7), the result of long-term radiation-stimulated annealing is obtaining the VO saturation concentration, which is determined by additional hot irradiation ($[VO](t \to \infty) = \lambda_V \tau$). In our experiment, we minimized the effect of additional irradiation by using samples with $[VO]_{RT} > \lambda_V \tau$ and lowered the electron irradiation energy to 0.8 MeV to reduce the efficiency of additional VO formation.[34,42]

Figure 4a shows the dependences of [VO] in Cz n-Si with P doping levels 1×10^{15} cm^{-3} (open symbols) and 5.5×10^{15} cm^{-3} (solid symbols) on the time of various radiation-heat treatments at 360 °C. Curve 1 represents hot irradiation with electrons with $E_e = 0.8$ MeV and $J = 1$ μA cm^{-2}. At the saturation stage $[VO]_{max} \approx 2.3 \times 10^{14}$ cm^{-3}. The solid line is the result of approximating the experimental data (symbols) by Equation (3), and the corresponding extracted value of τ is ≈ 840 s. Curves 2 and 4 represent isothermal annealing of samples previously irradiated at RT with simultaneous additional irradiation with $E_e \approx 0.8$ MeV electrons and $J = 1$ μA cm^{-2}. Solid lines represent the calculation using Equation (7) with the previously obtained value of $\tau = 840$ s (as for hot irradiation from curve 1). Curves 3 and 5 represent normal isothermal annealing. Solid lines are the calculation using Equation (2) and (7) with $E_a = 1.71$ eV and $\nu = 9.5 \times 10^9$ s^{-1} ($\tau \approx 4300$ s). Figure 4b compares the logarithm of the normalized VO concentration in Cz n-Si versus time during normal (curve 1) and radiation-stimulated (curve 2) isothermal annealing at 360 °C, when the contribution of additional irradiation is still small.

Key result from Figure 4, the VO defects were annealed much more efficiently (≈ 5 times) if annealing occurred simultaneously with the electron irradiation. This effect becomes more prominent when the $[VO]_{RT}$ is much larger than the contribution of

additional hot irradiation by 0.8 MeV electrons ($[VO]_{max} \approx 2.3 \times 10^{14}$ cm^{-3}). In addition (Figure 4b), in both cases, the annealing efficiency of VO complexes does not change with increasing P doping levels in Cz n-Si from 1×10^{15} cm^{-3} (open symbols) to 5.5×10^{15} cm^{-3} (solid symbols).

2.2. Radiation-Enhanced Annealing of VO Defects in Cz n-Si: Factor of the Radiation Ionization and a Possible Annealing Mechanism

2.2.1. Radiation-Induced Ionization as a Stimulating Factor for the Annealing of VO Defects

This section investigates the reasons for enhanced annealing of VO defects in Cz n-Si due to the intensity of electron irradiation. As J increases, at least two main processes are triggered: 1) the generation rate of free vacancies λ_V increases (see curve 1 in Figure 2a). In this case, it can be assumed that VO complexes can additionally disappear by capturing V (the concentration of which increases with increasing J) and transform into more complex defects; 2) the generation of nonequilibrium charge carriers $\Delta n \approx J$ increases due to radiation-induced ionization of Si samples. This may be the reason for the ionization-enhanced annealing of VO defects during their recharging.[43,44] To evaluate the contribution of these two processes in our experiments, we separated them from each other by irradiating electrons with different energies but the same irradiation intensity. In this case, the different E_e will affect the generation rate of free V and, accordingly, VO defects.[34,42] Along with this, the same J will create the same level of radiation-induced ionization in the Si samples. The energy losses for electrons with E_e in the range of ≈ 0.3–1.7 MeV in Si ($dE/dx \approx 360$ keV mm^{-1}) are losses on impact ionization and are almost independent of the initial E_e.[45,46] **Figure 5** compares time dependences of the [VO] in Cz n-Si for 1 MeV (curve 1) and 0.8 MeV (curve 2) electron irradiation of the same intensity ($J = 1$ μA cm^{-2}) at 360 °C. In
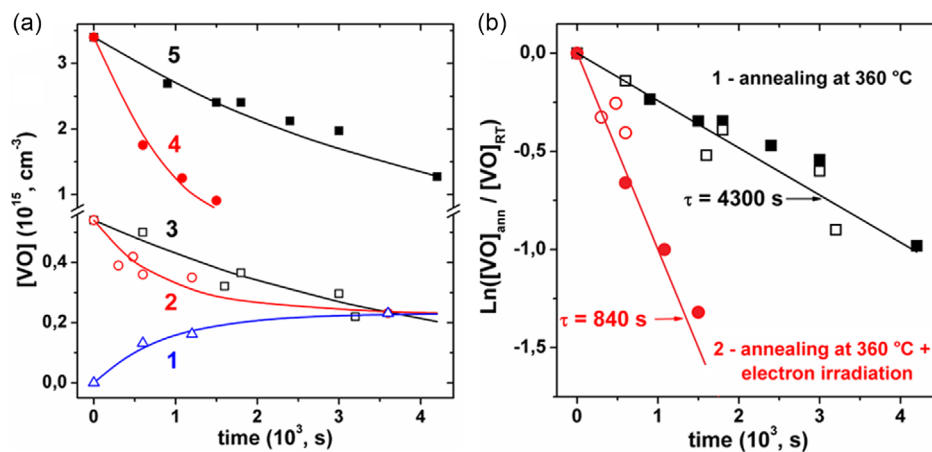

Figure 4. a) Dependences of the VO concentration in Cz n-Si on the time of various radiation-heat treatments at 360 °C: curve 1—hot irradiation with electrons with $E_e = 0.8$ MeV and $J = 1$ μA cm^{-2}; curves 2 and 4—isothermal annealing with simultaneous additional irradiation with $E_e = 0.8$ MeV electrons and $J = 1$ μA cm^{-2}; curves 3 and 5—normal isothermal annealing. b) The logarithm of the normalized VO concentration in Cz n-Si versus time during normal (curve 1) and radiation-stimulated (curve 2) isothermal annealing at 360 °C, when the contribution of additional irradiation is still small. Symbols—experimental data (solid symbols—samples with [P] $\approx 5.5 \times 10^{15}$ cm^{-3}; open symbols—samples with [P] $\approx 1 \times 10^{15}$ cm^{-3}). Each symbol in Figure 4 corresponds to a separate sample. Solid lines—calculated curves (see details in the text).
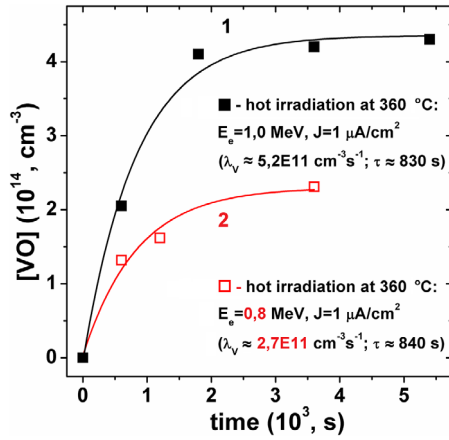
Figure 5. Comparison of dependences of the VO concentration in Cz n-Si versus the time of hot irradiation by electrons at 360 °C for $J = 1\,\mu\text{A cm}^{-2}$: curve 1—$E_e = 1$ MeV; curve 2—$E_e = 0.8$ MeV. Symbols—experiment; solid lines—approximation by Equation (3).

0.8 MeV electron irradiated samples, the initial rate of VO accumulation and the $[\text{VO}]_{\text{max}}$ (concentration in saturation) are almost 2 times smaller than in 1 MeV electron irradiated samples. Solid lines in Figure 5 represent the approximation of the experimental data by Equation (3), and the extracted values of the free V generation rate and the VO annealing time constant are as follows: $\lambda_V \approx 5.2 \times 10^{11}\,\text{cm}^{-3}\,\text{s}^{-1}$ and $\tau \approx 830$ s for samples irradiated with 1 MeV electrons and $\lambda_V \approx 2.7 \times 10^{11}\,\text{cm}^{-3}\,\text{s}^{-1}$ and $\tau \approx 840$ s for samples irradiated with 0.8 MeV electrons. That is, a decrease in E_e at a constant J leads to a decrease in λ_V by almost 2 times, while τ is the same in both cases. The consequence of this is a decrease in the initial rate of VO accumulation (from Equation (3), $d[\text{VO}]/dt(t \to 0) = \lambda_V$) and their concentration in saturation ($[\text{VO}]_{\text{max}} = \lambda_V \times \tau$, see Equation (4)). It means that changing the generation rate of free vacancies λ_V does not affect the annealing of VO defects. Therefore, the radiation-induced ionization should be a stimulating factor for the annealing of VO, which is confirmed by the equality of the annealing time constant τ for two groups of Si samples irradiated with different E_e electrons under conditions of the same radiation-induced ionization. In this context, it becomes clear that the additional radiation-induced ionization of the Si samples by electron irradiation is the main reason for the enhanced annealing of VO defects introduced into Cz n-Si at RT (see Figure 4).

2.2.2. A Possible Mechanism of Radiation-Enhanced Annealing of VO Defects

Thus, the increase in the generation rate of nonequilibrium carriers with increasing J is responsible for the decrease in τ for VO defects. Assume that the accelerated annealing of VO occurs due to their recharging (alternate capture of electrons and holes) similar to the normal ionization-enhanced diffusion mechanism or the athermal Bourgoin mechanism.[43,44] In this case, the concentration of both equilibrium and nonequilibrium charge carriers should affect the recharging rate and,

accordingly, the annealing rate of VO defects. In ref. [1], we calculated that the concentration of equilibrium electrons and holes in the samples increases from $n_0 = p_0 \approx 2.8 \times 10^{15}$ to $2.0 \times 10^{16}\,\text{cm}^{-3}$ with increasing temperature from 360 to 450 °C. This change in n_0 (p_0) is of the same order of magnitude as the concentration of nonequilibrium carriers created by the electron irradiation in our experiments, but the accelerated annealing of VO defects is not observed. As shown in Section 2.1.2, the activation energy and frequency factor for VO annealing are the same in the entire temperature range from 347 to 450 °C ($E_a \approx 1.71$ eV and $\nu \approx 9.5 \times 10^9\,\text{s}^{-1}$), and these values are in good agreement with those reported previously in the literature for the range 300–500 °C.[6,34] This means that it is necessary to find another mechanism for enhanced annealing of VO defects due to radiation-induced ionization.

To determine the parameters of this annealing process, we analyzed the kinetics of the VO accumulation at close temperatures of hot (347 and 360 °C) electron irradiation with $E_e = 1$ MeV and $J = 2\,\mu\text{A cm}^{-2}$, taking into account the pulsed irradiation mode. Then, the accelerated annealing of VO defects occurs during the action of the electron irradiation pulse, and their normal thermal annealing takes place between the pulses. Earlier, we obtained an expression to describe the kinetics of VO accumulation under high-temperature pulsed electron irradiation

$$[\text{VO}](t_{\text{irr}}) = \lambda_V \tau_1 \times \frac{\exp\left(-\frac{t_{\text{off}}}{\tau_2}\right) \times \left(1 - \exp\left(-\frac{t_p}{\tau_1}\right)\right)}{1 - \exp\left(-\frac{t_{\text{off}}}{\tau_2}\right) \times \exp\left(-\frac{t_p}{\tau_1}\right)} \times \left(1 - \exp\left(-\left[\frac{t_{\text{off}}}{\tau_2} + \frac{t_p}{\tau_1}\right] \times \frac{t_{\text{irr}}}{t_{\text{off}} + t_p}\right)\right)$$

(8)

where τ_1 and τ_2 are the annealing time constant of VO defects during the action of the irradiation pulse and between the pulses, respectively; t_p is the pulse duration; t_{off} is the time interval between pulses.[39]

Provided that $[t_{\text{off}}/\tau_2 + t_p/\tau_1] \times t_{\text{irr}}/(t_{\text{off}} + t_p) \gg 1$, the dependence $[\text{VO}](t_{\text{irr}})$ reaches saturation, and then from Equation (8), we obtain

$$[\text{VO}]_{\text{max}} = \frac{\lambda_V}{(t_{\text{off}}/t_p)/\tau_2 + 1/\tau_1}$$

(9)

where $(t_{\text{off}}/t_p)/\tau_2$ and $1/\tau_1$ are the annealing rate of VO between the pulses and during the action of the irradiation pulse, respectively.

In Equation (8) and (9), λ_V and τ_1 are unknown J-dependent fitting parameters. From another experiment in Figure 3, we determined the normal annealing rate of VO defects $1/\tau_2 \approx 9.5 \times 10^9 \times \exp(-1.71/kT)$. The t_p and t_{off} are known technical parameters of the electron accelerator ($t_{\text{off}}/t_p \approx 10^3$). **Figure 6** shows dependences of the VO concentration on the time of hot 1 MeV electron irradiation at 360 °C (curve 1) and 347 °C (curve 2) with $J = 2\,\mu\text{A cm}^{-2}$. Solid lines correspond to the best fit of theory (Equation (8)) to the experimental data (symbols). **Table 2** shows the values of parameters λ_V, $1/\tau_1$ and $(t_{\text{off}}/t_p)/\tau_2$, which characterize the dependences $[\text{VO}](t_{\text{irr}})$ in Figure 6 (solid lines).
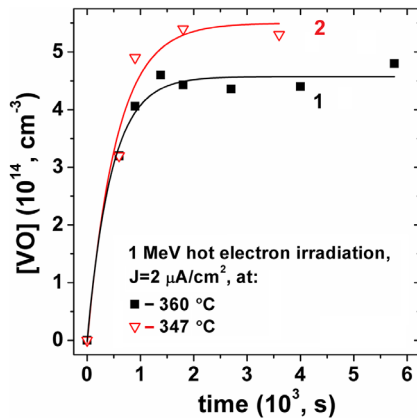
Figure 6. Dependences of the VO defects concentration in Cz n-Si on the time of hot irradiation by 1 MeV electrons with $J = 2\,\mu A\,cm^{-2}$ at 360 °C (curve 1) and 347 °C (curve 2). Symbols—experiment; solid lines—fitting using Equation (8) (see text for details).

Table 2. Values of the parameters λ_V, $1/\tau_1$, and $(t_{off}/t_p)/\tau_2$, which characterize dependences of the VO accumulation in Cz n-Si at high-temperature electron irradiation.

Irradiation conditions			Free vacancies generation rate	VO annealing rate	
E_e [MeV]	J [$\mu A\,cm^{-2}$]	T_{irr} [°C]	λ_V [$\times 10^{14}\,cm^{-3}\,s^{-1}$]	$1/\tau_1$ [s^{-1}]	$(t_{off}/t_p)/\tau_2$ [s^{-1}]
1	2	347	10.0	1.66	$10^3/8300$ ≈ 0.12
1	2	360	10.2	2.0	$10^3/4300$ ≈ 0.23

Assuming that $1/\tau_1$ exhibits a thermally activated Arrhenius behavior for electron irradiation at 347 and 360 °C, we calculated the activation energy and frequency factor for accelerated annealing of VO defects using Equation (2) with the values for $1/\tau_1$ that are presented in Table 2: $E_a = 0.5 \pm 0.05$ eV and $\nu \approx 1.9 \times 10^4$ s^{-1} ($\nu \approx 7.6 \times 10^3$–$4.8 \times 10^4$ s^{-1}). Thus, we obtained that the activation energy for VO annealing decreases from ≈ 1.7 (the normal annealing) to ≈ 0.5 eV (the enhanced annealing) due to radiation-induced ionization of the silicon crystal.

Figure 7 shows a scheme of the band structure of silicon. The radiation-induced ionization energy in silicon is ≈ 3.6 eV per excited electron–hole pair, which is much larger than the Si bandgap (≈ 1.1 eV).[46] Therefore, excited electrons can fall into the high-energy valleys of Si.

We assumed that when such electrons are captured by the VO complexes, defects receive energy, which significantly reduces the activation energy of their annealing. In Cz Si, the dominant annealing mechanism for VO is the trapping of mobile VO by interstitial oxygen (O_i) atom, thus forming VO$_2$.[6,15,18–20] We consider that the captured electron stimulates the jump of the VO defect to the neighboring position in the crystal. As a result, the reaction VO + $O_i \rightarrow$ VO$_2$ will occur faster. Specifically, the reason for the accelerated annealing can be the capture of electrons from the L_1 valley by VO defects (see Figure 7). The
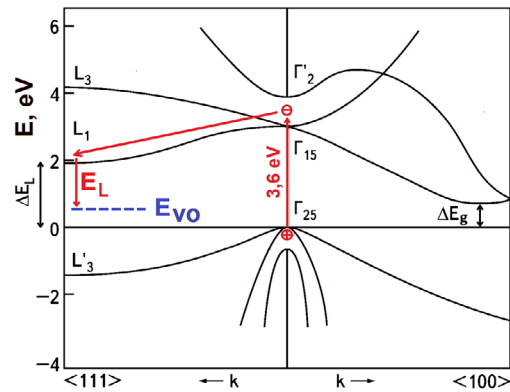

Figure 7. Scheme of the band structure of silicon and the capture of electrons from the high-energy valley of silicon (L_1) by VO defects.

minimum of the conduction band at the point L_1 has the energy $\Delta E_L \approx 2.0$ eV relative to the highest point of the valence band. In this case, the activation energy for accelerated annealing of VO defects ($E^*_{a(VO)}$) is expressed as $E^*_{a(VO)} = E_{a(VO)} - E_L$, where $E_{a(VO)} \approx 1.7$ eV is the activation energy for normal (thermal) annealing of VO defects and E_L is the energy transferred to the VO defects during the capture of electrons from the L_1 valley. The energy E_L is given by the relation $E_L = \Delta E_L - (\Delta E_g - E_{VO})$, where ΔE_g is the energy of the Si bandgap and $E_{VO} = 0.17$ eV is the electronic level of VO defects. Then, we have that $E^*_{a(VO)}$ is in the ≈ 0.45–0.65 eV range, taking into account the temperature dependence of ΔE_g.[47] The obtained value of $E^*_{a(VO)}$ is practically identical with the activation energy for accelerated annealing of VO complexes, calculated from the experimental data in Figure 6. Thus, in our model, the $1/\tau_1$ is given by the relation

$$\frac{1}{\tau_1} = \nu(J) \times \exp\left(-\frac{0.5}{kT}\right) \quad (10)$$

where $\nu(J)$ is the frequency factor that depends on the electron irradiation intensity and is determined by the annealing mechanism of VO defects.

Figure 8 (symbols) shows calculated values ν depending on the intensity of pulsed 1 MeV electron irradiation at 360 °C. First, we obtained the dependences of $1/\tau_1(J)$ and $\lambda_V(J)$ ($\lambda_V/J = 7.9 \times 10^{-2}$ cm^{-1}) by approximating the experimental data in Figure 1 by Equation (8). Then, we calculated the dependence of $\nu(J)$ using Equation (10) from the dependence of $1/\tau_1(J)$. As can be seen from Figure 8, the frequency factor ν increases by more than an order of magnitude (accordingly, the annealing time constant τ_1 decreases) with increasing the irradiation intensity by an order of magnitude, which indicates an accelerated annealing of VO defects. The dependence of $\nu(J)$ increases almost linearly in the investigated range of J. Solid line in Figure 8 is a linear approximation of $\nu(J) = A \times J$. The corresponding extracted value of the parameter A for hot electron irradiation at 360 °C is $\approx 1.4 \times 10^{-12}$ cm^2 (for [VO]$_{max} = 5 \times 10^{14}$ cm^{-3}).
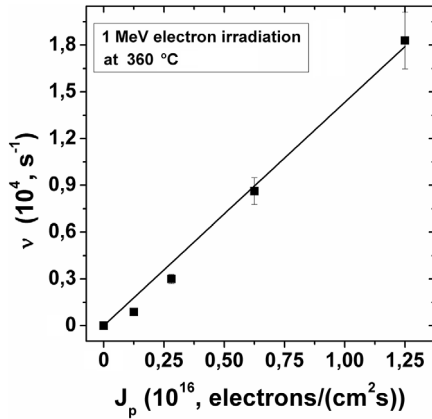
Figure 8. Dependence of the ν on the intensity of pulsed 1 MeV electron irradiation at 360 °C. Symbols are the calculated values of ν (see text for details). Solid line is a linear approximation.

Assuming that the dependence of $\nu(J)$ is also linear for hot 1 MeV electron irradiation of samples at 347 °C ($J = 2\,\mu A\,cm^{-2}$) and 450 °C ($J = 8\,\mu A\,cm^{-2}$), we calculated the corresponding values of the constants $A_{347} \approx 1.55 \times 10^{-12}\,cm^2$ and $A_{450} \approx 4.1 \times 10^{-12}\,cm^2$ (for $[VO]_{max}$ of 8×10^{13} and $9.5 \times 10^{13}\,cm^{-3}$, A_{450} is $\approx 2.3 \times 10^{-12}\,cm^2$ and $\approx 1.8 \times 10^{-12}\,cm^2$, respectively). Then, the analytical form of Equation (9) for $[VO]_{max}$ in samples after hot 1 MeV electron irradiation in the temperature range ≈ 300–500 °C is given by the relation

$$[VO]_{max} = \frac{7.9 \times 10^{-2} \times J_p}{9.5 \times 10^{12} \times \exp\left(-\frac{1.71}{kT}\right) + A \times J_p \times \exp\left(-\frac{0.5}{kT}\right)} \tag{11}$$

Figure 9 shows the dependence of $[VO]_{max}$ on the intensity of pulsed 1 MeV electron irradiation J_p for several temperatures. Solid lines in Figure 9 correspond to the approximation of experimental data (symbols) with Equation (11). We see that the theoretical curves coincide satisfactorily with the experimental data.
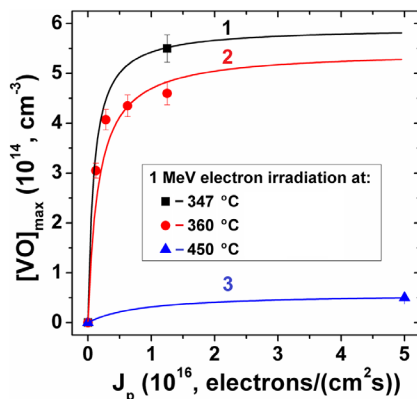

Figure 9. Dependence of $[VO]_{max}$ in Cz n-Si ($[P] \approx 1 \times 10^{15}\,cm^{-3}$) on the intensity of pulsed 1 MeV electron irradiation J_p for 347 °C (curve 1), 360 °C (curve 2), and 450 °C (curve 3). Symbols—experiment; solid lines—fitting using Equation (11) (see text for details).

3. Conclusion

We have studied in detail the effect of radiation-enhanced annealing of VO complexes in Cz n-Si, which occurs under the influence of electron irradiation of a certain intensity. It is shown that: 1) During hot 1 MeV electron irradiation of samples at temperatures of 347, 360, 450, and 535 °C, which leads to the simultaneous generation and annealing of VO complexes, the intensity of this irradiation can significantly accelerate the annealing of the created VO defects. The maximum concentration of VO defects ($[VO]_{max}$) accumulated in this case increases with increasing irradiation intensity and decreases with increasing temperature of the samples during irradiation. Accelerated annealing of VO slows down sharply the growth rate of $[VO]_{max}$ as a function of J. 2) Also, the VO defects introduced in Cz n-Si at RT can anneal faster if the annealing is accompanied by additional electron irradiation of a certain intensity. 3) The radiation-accelerated annealing of VO is characterized by a decrease in the activation energy from ≈ 1.7 to ≈ 0.5 eV. 4) Using electron irradiation with different energies (0.8 and 1 MeV) and same intensities, we obtained experimental results indicating that radiation-induced ionization of Si samples causes accelerated annealing of VO defects. We propose a model of the possible mechanism of this effect based on the assumption that the sample electrons are excited to the high-energy valley of Si (L_1) under the action of electron irradiation. At the capture of such electrons, VO complexes receive energy that significantly reduces the activation energy of their annealing.

4. Samples and Experimental Methods

Phosphorus-doped Cz n-Si with an initial concentration of free electrons (n_0) $\approx 1 \times 10^{15}\,cm^{-3}$, $5.5 \times 10^{15}\,cm^{-3}$, and $2 \times 10^{16}\,cm^{-3}$ was studied. In all samples, the concentrations of interstitial oxygen atoms ($[O_i]$) were in the range of $(6$–$8) \times 10^{17}\,cm^{-3}$ and the concentrations of substitutional carbon atoms ($[C_s]$) $\leq 5 \times 10^{16}\,cm^{-3}$.

A pulsed electron accelerator with the following characteristics was used for irradiation: electron energy E_e of 1 and ≈ 0.8 MeV, pulse duration $t_p = 3.3\,\mu s$, and duty cycle $s = 10^3$. The samples were irradiated at RT, 347, 360, 450, and 535 °C with fluences (Φ) ranging from 2.5×10^{15} to $1.8 \times 10^{17}\,cm^{-2}$. The average current intensities of electron irradiation were in the range of $J = 0.2$–13.5 $\mu A\,cm^{-2}$ (accordingly, the pulse flux density was in the range of $J_p = 1.25 \times 10^{15}$–$8.5 \times 10^{16}$ electrons $cm^{-2}\,s^{-1}$). For samples irradiated at 347 and 360 °C with $J = 0.2$–2 $\mu A\,cm^{-2}$, we used a special furnace for heating. The heating of samples up to 450 and 535 °C was done in situ by the electron beam with J of 8 and 13.5 $\mu A\,cm^{-2}$, respectively. The technique of such an experiment was described by us earlier.[3,4,9,10]

To determine the parameters of normal (influence of temperature only) and accelerated (simultaneous influence of temperature and additional electron irradiation) annealing of VO defects, isothermal annealing of samples irradiated at RT was carried out in a furnace at the same temperatures as for hot irradiation. The concentration of VO complexes after each stage of irradiation or annealing was determined from the temperature dependencies of the Hall effect. Details of this experimental procedure are described in previous works.[1,32] For 1 MeV hot electron irradiation at 450 and 535 °C, the VO concentration was determined by using the deep-level transient spectroscopy in our previous studies.[4,9,10] The relative error of VO concentration measurement is estimated to be <10%.

Conflict of Interest

The authors declare no conflict of interest.

Data Availability Statement

The data that support the findings of this study are available from the corresponding author upon reasonable request.

[1] M. M. Kras'ko, A. G. Kolosiuk, V. B. Neimash, V. Y. Povarchuk, I.S. Rogutskyi, A.O. Goushcha, *J. Mater. Res.* **2021**, *36*, 1646.

[2] D. C. Schmidt, B. G. Svensson, J. L. Lindström, S. Godey, E. Ntsoenzok, J. F. Barbot, C. Blanchard, *J. Appl. Phys.* **1999**, *85*, 3556.

[3] V. B. Neimash, M. M. Kras'ko, A. M. Kraitchinskii, *Ukr. J. Phys.* **2002**, *47*, 50.

[4] V. Neimash, M. Kras'ko, A. Kraitchinskii, V. Voytovych, V. Tishchenko, E. Simoen, J. M. Rafi, C. Claeys, J. Versluys, O. De Gryse, P. Clauws, *Phys. Status Solidi A* **2004**, *201*, 509.

[5] J. L. Lindström, L. I. Murin, T. Hallberg, V. P. Markevich, B. G. Svensson, M. Kleverman, J. Hermansson, *Nucl. Instrum. Methods Phys. Res. B* **2002**, *186*, 121.

[6] V. Quemener, B. Raeissi, F. Herklotz, L. I. Murin, E. V. Monakhov, B. G. Svensson, *J. Appl. Phys.* **2015**, *118*, 135703.

[7] J.-G. Xu, F. Lu, H.-H. Sun, *Phys. Rev. B* **1988**, *38*, 3395.

[8] J. Lalita, B. G. Svensson, C. Jagadish, *Nucl. Instrum. Methods Phys. Res.* **1995**, *96*, 210.

[9] E. Simoen, J. M. Rafi, C. Claeys, V. Neimash, A. Kraitchinskii, M. Kras'ko, V. Tishchenko, V. Voytovych, J. Versluys, P. Clauws, *Jpn. J. Appl. Phys.* **2003**, *42*, 7184.

[10] E. Simoen, C. Claeys, V. Neimash, A. Kraitchinskii, M. Kras'ko, V. Tishchenko, V. Voytovych, *Solid State Phenom.* **2004**, *95–96*, 367.

[11] V. P. Markevich, A. R. Peaker, S. B. Lastovskii, V. E. Gusakov, I. F. Medvedeva, L. I. Murin, *Solid State Phenom.* **2010**, *156–158*, 299.

[12] H. Ohyama, K. Takakura, H. Matsuoka, T. Jono, E. Simoen, C. Claeys, J. Uemura, T. Kishikawa, *J. Mater. Sci.: Mater. Electron.* **2003**, *14*, 437.

[13] H. Ohyama, K. Hayama, K. Takakura, T. Miura, K. Shigaki, T. Jono, E. Simoen, A. Poyai, C. Claeys, *J. Mater. Sci.: Mater. Electron.* **2003**, *14*, 451.

[14] M. Nakabayashi, H. Ohyama, N. Hanano, E. Simoen, C. Claeys, K. Takakura, T. Iwata, T. Kudou, M. Yoneoka, *J. Mater. Sci.: Mater. Electron.* **2005**, *16*, 463.

[15] J. W. Corbett, G. D. Watkins, R. S. Mc Doland, *Phys. Rev.* **1964**, *135*, A1381.

[16] C. A. Londos, L. G. Fytros, G. J. Georgiou, *Defect Diffus. Forum* **1999**, *171–172*, 1.

[17] L. I. Murin, E. A. Tolkacheva, S. B. Lastovskii, V. P. Markevich, J. Mullins, A. R. Peaker, B. G. Svensson, *Phys. Status Solidi A* **2019**, *216*, 1800609.

[18] J. L. Lindström, L. I. Murin, V. P. Markevich, T. Hallberg, B. G. Svensson, *Phys. B* **1999**, *273–274*, 291.

[19] X. Yu, L. Chen, P. Cheng, D. Yang, *Appl. Phys. Express* **2012**, *5*, 021302.

[20] B. G. Svensson, J. L. Lindström, *Phys. Rev. B* **1986**, *34*, 8709.

[21] S. Jin, P. Wang, Y. Qin, C. Cui, D. Yang, X. Yu, *J. Phys.: Condens. Matter.* **2020**, *32*, 275702.

[22] A. Abdurrazaq, A. T. Raji, W. E. Meyer, *Silicon* **2021**, *13*, 1969.

[23] L. I. Murin, J. L. Lindström, B. G. Svensson, V. P. Markevich, A. R. Peaker, C. A. Londos, *Solid State Phenom.* **2005**, *108–109*, 267.

[24] V. V. Voronkov, R. Falster, C. A. Londos, *J. Appl. Phys.* **2012**, *111*, 113530.

[25] C. A. Londos, A. Chroneos, E. N. Sgourou, I. Panagiotidis, T. Angeletos, M. S. Potsidi, *Appl. Sci.* **2022**, *12*, 8151.

[26] P. Dong, X. Yu, L. Chen, X. Ma, D. Yang, *J. Appl. Phys.* **2017**, *122*, 095704.

[27] P. Dong, P. Yang, M. Xie, *Radiat. Eff. Defects Solids* **2018**, *173*, 1018.

[28] Y. Qin, P. Wang, S. Jin, C. Cui, D. Yang, X. Yu, *Mater. Sci. Semicond. Process.* **2019**, *98*, 65.

[29] A. Chroneos, E. N. Sgourou, C. A. Londos, U. Schwingenschlögl, *Appl. Phys. Rev.* **2015**, *2*, 021306.

[30] G. D. Watkins, J. W. Corbett, *Phys. Rev.* **1961**, *121*, 1001.

[31] E. Sonder, L. C. Templeton, *J. Appl. Phys.* **1960**, *31*, 1279.

[32] V. B. Neimash, V. V. Voitovych, M. M. Kras'ko, A. M. Kraitchinskii, O. M. Kabaldin, Yu. V. Pavlovs'kyi, V. M. Tsmots, *Ukr. J. Phys.* **2005**, *50*, 1273.

[33] L. F. Makarenko, *Semicond. Sci. Technol.* **2001**, *16*, 619.

[34] S. D. Brotherton, P. Bradley, *J. Appl. Phys.* **1982**, *53*, 5720.

[35] M. Kras'ko, A. Kolosiuk, V. Voitovych, V. Povarchuk, *Phys. Status Solidi A* **2019**, *216*, 1900290.

[36] M. Kras'ko, A. Kolosiuk, V. Voitovych, V. Povarchuk. *Phys. Status Solidi A* **2021**, *218*, 2100209.

[37] M. Kras'ko, A. Kolosiuk, V. Povarchuk, V. Voitovych. *Phys. Status Solidi A* **2024**, *221*, 2400300.

[38] A. Kraitchinskii, A. Kolosiuk, M. Kras'ko, V. Neimash, V. Voitovych, V. Makara, R. Petrunya, S. Putselyk, *Radiat. Eff. Defects Solids* **2011**, *166*, 445.

[39] M. Kras'ko, A. Kraitchinskii, A. Kolosiuk, V. Neimash, V. Voitovych, V. Makara, R. Petrunya, V. Povarchuk. *Solid State Phenom.* **2011**, *178–179*, 404.

[40] K. Wu, X. Lv, D. Zou, Y. Lu, J. Li, Y. Zhao, *Nucl. Instrum. Methods Phys. Res. A* **2022**, *1034*, 166743.

[41] M. Mikelsen, J. H. Bleka, J. S. Christensen, E. V. Monakhov, B. G. Svensson, J. Härkönen, B. S. Avset, *Phys. Rev. B* **2007**, *75*, 155202.

[42] R. Radu, I. Pintilie, L. C. Nistor, E. Fretwurst, G. Lindstroem, L. F. Makarenko, *J. Appl. Phys.* **2015**, *117*, 164503.

[43] J. C. Bourgoin, J. W. Corbett, H. L. Frisch, *J. Chem. Phys.* **2015**, *59*, 4042.

[44] J. C. Bourgoin, J. W. Corbett, *Phys. Lett.* **1972**, *38A*, 135.

[45] S. Banerjee, A. Caner, S. Dutta, A. Khanov, F. Palla, G. Tonelli, (Preprint) CMS Note, CMS-NOTE-1999-056, v1, submitted: October **1999**.

[46] C. Claeys, J. Vanhellemont, *Radiat. Eff. Defects Solids* **1994**, *127*, 267.

[47] V. Alex, S. Finkbeiner, J. Weber, *J. Appl. Phys.* **1996**, *79*, 6943.